

SAND91-1263C

SAND--91-1263C

DE92 001621

PROTOTYPE DISH TESTING AND ANALYSIS AT SANDIA NATIONAL LABORATORIES¹

J. W. Grossman, R.M. Houser, and W.W. Erdman
Divisions 6216 and 6215
Sandia National Laboratories
Albuquerque, New Mexico 87185

Abstract

During the past year, Sandia National Laboratories performed on-sun testing of several dish concentrator concepts. These tests required different approaches, and a variety of tests was undertaken at the National Solar Thermal Test Facility (NSTTF). Two of the tests were performed in support of the DOE Concentrator Receiver Development Program. The first was on-sun testing of the single-element stretched-membrane dish; this 7-meter diameter dish uses a single preformed metal membrane with an aluminized polyester optical surface and shows potential for future dish-Stirling systems. The next involved two prototype facets from the Faceted Stretched-Membrane Dish Program. These facets, representing competitive design concepts, are closest to commercialization. The final test in this series was done at the request of NASA. Five 1-meter triangular facets were tested on-sun as part of the development program for a solar dynamic system on Space Station Freedom.

While unique in character, all the tests utilized the Beam Characterization System (BCS) as the main measurement tool and all were analyzed using the Sandia-developed CIRCE2 computer code. The BCS is used to capture and digitize an image of the reflected concentrator beam that is incident on a target surface. The CIRCE2 program provides a computational tool, which when given the geometry of the concentrator and target as well as other design parameters will predict the flux distribution of the reflected beam. One of these parameters, slope error, is the variable that has a major effect in determining the quality of the reflected beam. The methodology used to combine these two tools to predict uniform slope errors for the dishes is discussed in this document.

As the Concentrator Development Programs continue, Sandia will test and evaluate two prototype dish systems. The first, the faceted stretched-membrane dish, is expected to be tested in 1992, followed by the full-scale single-element stretched-membrane dish in 1993. These tests will use the tools and methodology discussed in this document.

¹ This work at Sandia National Laboratories, Albuquerque, New Mexico, is supported by the U. S. Department of Energy under contract DE-AC04-76DP00789 and the National Aeronautics and Space Administration under Interagency Agreement No. C-31000-M.

1. Introduction

The National Solar Thermal Test Facility (NSTTF) is operated by Sandia National Laboratories for the U. S. Department of Energy's Solar Thermal Program. The NSTTF, located on Kirtland Air Force Base in Albuquerque, NM, is capable of supporting experiments requiring high heat fluxes and/or specific flux distributions that can vary spatially and with time [1,2]. A wide range of solar experiments has been conducted, including the testing of central receivers (water, air, sodium, and salt), the development of solar concentrators (trough, heliostat and dish), the simulation of nuclear thermal flash, the effects of aerodynamic heating, evaluation of thermophysical properties of materials, and astronomical observations.

The three primary test facilities located at the NSTTF are the central receiver test facility, point-focus parabolic dishes and solar furnaces. The central receiver test facility comprises 222 computer-controlled heliostats that can reflect the sun's energy to a number of locations along a 200-foot tall tower. The facility can provide up to 5 MW of thermal power at peak fluxes to 2600 kW/m². Two point-focus test bed concentrators are capable of providing 75 kW_t each with peak fluxes up to 150 kW/m². Since the concentrators are made of 220 facets each, it is possible to alter the facet alignments to achieve a range of flux distributions and power levels. Two solar furnaces, capable of providing 16 and 65 kW_t, are also available for solar testing where experiments require that the focal point not move and/or that the power level be adjustable during the test.

The more important features of the NSTTF are the test support and experience that is available there. Modern data acquisition, control and diagnostic systems are available for the use of the experimenter. In addition, specialized instrumentation such as the Beam Characterization System (BCS), used to measure the solar intensity profiles produced by all types of concentrators, has been developed at the NSTTF. Sandia has also developed several computer codes, HELIOS [3] and CIRCE[4] and CIRCE2 [5], to model solar concentrator and receiver optical performance.

CIRCE2 has been used to predict performance values, such as peak and total power, for the prototype concentrators being tested with the BCS. Comparisons of the theoretical image to the actual image have to date been subjective, relying on visual judgement.

Sandia has recently completed testing of three different concentrators. Each of these tests is unique in the approach used for testing, and therefore is a good example to illustrate the adaptability of the BCS and the flexibility of CIRCE2. During the analysis of the results, we employed a methodology being developed for analytically comparing the real image measurements with the theoretical predictions. This methodology, while still in development, provides a quantitative measurement of image disparity, removing much of the subjectivity from the image analysis and enhancing our ability to predict receiver performance.

2. Beam Code System

The primary test instrumentation used to measure the on-sun flux density distributions produced by concentrators is Sandia's Beam Characterization System (BCS). A schematic diagram of the system is shown in Figure 1. The BCS comprises a Lambertian target plane with an internal flux gauge, a video camera with neutral density filters, and a computer system with a frame grabber that digitizes the video image, displays it on a monitor and stores it for later evaluation. A software package called Beamcode[®], developed by Big Sky Software and enhanced by them for Sandia, is used to produce flux-density contour plots. The digitized image is stored and later processed to provide plots, total beam power, and the flux-density distribution. The software is capable of displaying up to sixteen intensity ranges with a color assigned to each range. It is also capable of creating various apertures (circular, square, rectangular), determining peak intensity values, locating the centroid of an image, and creating various graphical displays of the image (3-D surfaces, contours, profiles, and histograms).

The target, onto which the solar image from a concentrator is directed, must be Lambertian -- it must scatter the incident light uniformly (intensity varies with cosine angle) in all directions. Target selection is based on the estimated peak flux of the concentrator. A high-temperature insulation board is used as the target when the estimated peak flux is below 40 kW/m². For fluxes above this level, a water-cooled target with a plasma-sprayed aluminium oxide coating is used. Previous laboratory measurements of these surfaces have shown them to be nearly Lambertian. Calibrated flux gauges are located at one or two points (depending on the target configuration) on

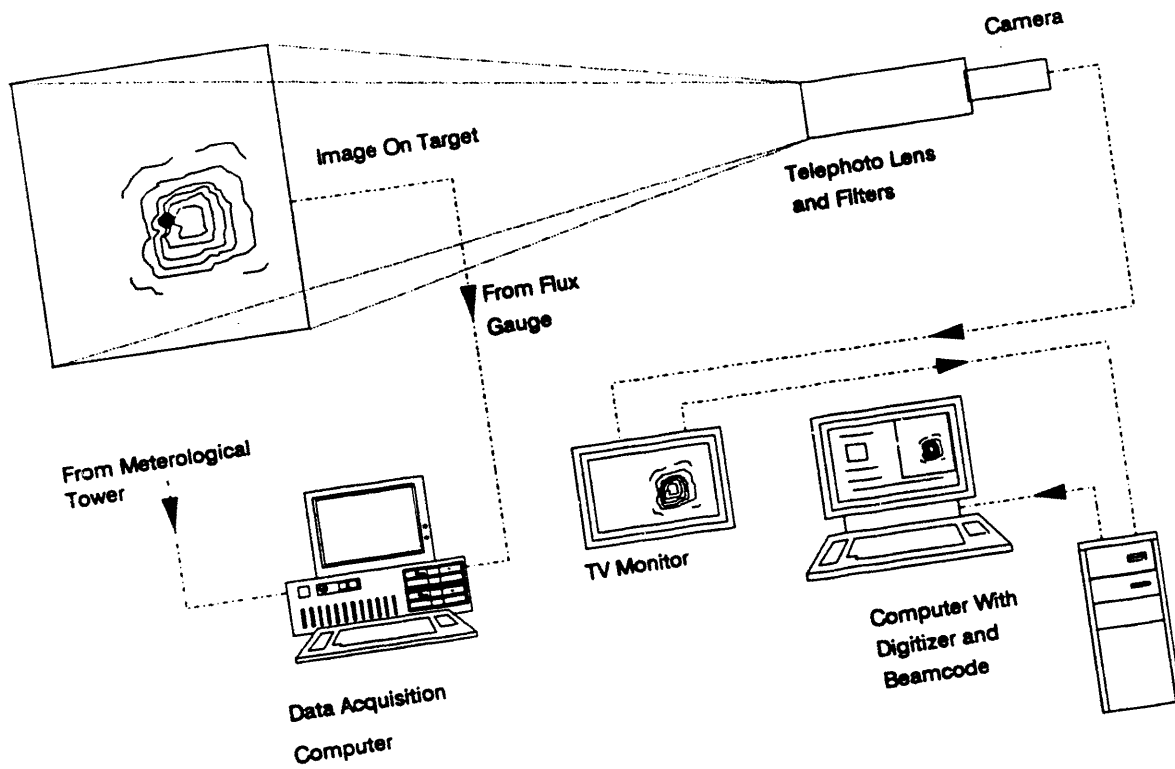


Figure 1. Beam Characterization System Schematic

the target surface. They provide a direct measurement of the flux density at their location within the reflected flux-density profile so that the measured gray-scale level can be calibrated to solar intensity. Lower flux densities are measured with normal incidence pyroheliometers and higher flux intensities are measured with water-cooled flux gauges.

The video camera has a visual spectral response, a wide dynamic range, high resolution, zero geometric distortion, and no lag or image retention. Standard "C" mount lenses with neutral density filters are used on the camera to adjust the intensity levels viewed by the camera to avoid saturation. The video frame grabber and digitizer provides a spatial resolution up to 240 by 240 pixels with 256 grey-scale intensity levels. Images can be captured at rates up to 60 per second.

As part of the test procedure for the BCS, a nonilluminated image of the target is made prior to the actual test sequence. This image is subtracted from each test image by the software as a means of reducing "background noise". As a result, each pixel in the digitized test image has an integer value of 0 to 255 relative to the 0 pixel level.

2.1 Uncertainties In The Measurements

The uncertainties for the measurements made during on-sun testing are listed in Table 1.

Measurement Variable	Measurement Uncertainties	Measured Uncertainty
Time of Day	± 5 Seconds	
Ambient Temperature	± 0.28 °C	
Wind Speed	± 5 % of reading	
Wind Direction	± 10 % of reading	
Solar Radiation	± 2 % of reading	
Target Flux	± 8 % of maximum value	
Target-to-Facet Distance	± 6.4 mm	
Azimuth and Elevation	± 0.5 Degrees	
Reflectivity	± 2 % of reading	

For the analysis, the most important reduced measurement made in these tests is the scale factor that is developed to establish the flux levels associated with the measured flux-density distributions. There are several types (normal

incident pyroheliometers and circular foil heat flux gauges) and ranges of flux gauges employed in testing. As mentioned above, gauge selection is based on the estimated peak flux of the test concentrator. This measurement is the first uncertainty in the chain of measurements that leads to a flux uncertainty. Also, part of this chain is the uniformity of the neutral density filters, the correction for the angle between the camera view and the target normal, and the uncertainty of the size and intensity of a pixel in the final distribution. Our estimate is that the measured flux-densities are within $\pm 8\%$ of the reported peak-flux value. Lower flux values have less resolution because of the fewer number of pixels that represent them in the given distribution.

3. The CIRCE2 Computer Code

CIRCE2 is a dish-receiver code adapted from HELIOS, a code developed in the late 1970s for central receiver systems (in Greek mythology, Circe is the daughter of Helios). The solution technique employed in CIRCE is the same as in HELIOS; that is, the concentrator errors are convolved with the sunshape to produce the flux-density distribution on an arbitrary target plane. Input to CIRCE2 is a file containing the parameters listed below arranged in a specific sequence. A short program creates the file and prompts the user for the required input.

3.1 CIRCE2 Input

Sunshape

The sunshape input can be either Gaussian, a uniform disk with any of six limb-darkening options, or a user-specified tabular input. A clear-day, tabular sunshape, measured at the NSTTF, was used for all CIRCE2 simulations reported in this document.

Sun, Dish, and Target Orientation

In CIRCE2, the position of the sun is assumed to be directly overhead of an upward facing dish (Figure 2 illustrates the CIRCE2 coordinate system). Inputs to the program, however, allow for alternate specification of the position vectors for the sun, the target, and the concentrator. The concentrator or individual facet aim-points (50) or the normal vectors (250) can be specified. When concentrator aim-points are specified they are based on an on-axis sun position. The effect of the concentrator tracking errors can, therefore, be analyzed by specifying an off-axis sun position and aim-points. Specification of facet normals allows

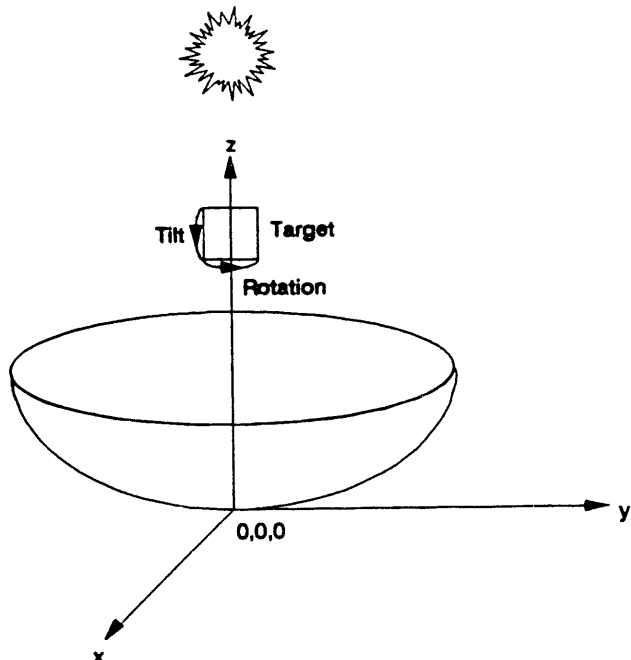


Figure 2. CIRCE2 Default Geometry.

for independent adjustment of not only the normals but also sun position. The target can also be rotated and tilted to any desired offset. This flexibility allows the modeling of many diverse test configurations. By transforming the test coordinate system to CIRCE2 coordinates, the program inputs pattern the actual positions of the sun, target, and concentrator.

Error Parameters

Up to five different reflector errors can be input to the code as either one-dimensional (circular normal) or two-dimensional (elliptic normal) errors. A single, circular-normal slope error was used to model the performance of all the concentrators described in this document. The 1 standard- deviation value of the slope error is input to the code to model its distribution. The slope error is varied until a prescribed match between the predicted and measured peak flux is found.

Convolution

The convolution of the errors and the sunshape can be one- or two-dimensional and either numerically or analytically calculated. A two-dimensional numerical convolution is used for the concentrators because of the offsets and the tabular sun input.

Target Shadowing

Target shadowing or blockage of the reflective surface can be input as a percentage of the concentrator/facet projected area or computed

internally by overlaying a projection of the target on the facets. Target shadowing is neglected in the tests where no shadowing occurred.

Reflector Types

CIRCE2 can model either continuous surfaces or faceted concentrators. The reflectance of the optical surface is also an input variable. The test items were all single elements, and therefore, modeled as continuous surfaces. Reflectivity measurements taken on each item were used as input to the models.

Facet Shape

CIRCE2 can support rectangular, circular, or triangular reflector shapes. Selection of the shape was based on the test item.

Facet Contour

The facet contour may be parabolic, spherical, flat, or an arbitrary user-input shape. Selection of the contour was based on the concentrator.

3.2 CIRCE2 Slope Error

The CIRCE2 code models the facet as a contour of revolution; that is, the reflector surface is axisymmetric. The primary assumption in the code is that the slope errors are randomly distributed over the surface of the reflector. In fact, this is rarely the case since fabrication techniques often result in organized departures of the facet contour from design. Nonetheless, the uniformly distributed slope error used in CIRCE2 is useful as a figure-of-merit for comparing the relative performance of the concentrators tested in this study. Furthermore, the slope error that is found to best represent the concentrator performance in a given configuration can be used in CIRCE2 to predict its performance for any modeled configuration.

4. Comparing Images

One method for using CIRCE2 and the BCS for analyzing test results has been to vary the slope error in CIRCE2 until the peak flux determined by the code closely matches the value ascertained from the image data. Intensities reported by Beamcode[®] are relative to the zero background of the image. To begin the analysis, flux intensities are determined from the flux gauge measurements and the beam image. Flux gauge locations in the target appear as a hole in the image surface. Viewing profiles of the hole with the BCS software provides a means for determining the relative intensity of the pixels at the edge of the gauge location. By interpolating, a relative intensity for

the pixel at the center of the gauge can be determined. This value is ratioed to the measured flux, resulting in a scale factor for the entire image array.

The BCS software allows input of the factor to scale the image to the actual peak power and includes some functions to provide graphical and digital information about the image. However, the size of the files is much larger than the 25-by-25 flux distribution array generated by CIRCE2, so visual comparisons of the image contours or profiles for analysis have been the general practice. This is, naturally, a fairly subjective method, which to date has been acceptable since the slope error is figure-of-merit and is not usually reported with more than two significant digits.

With these limitations in mind, development of a more rigorous comparison method was begun. The first step was converting the binary image data file, which represents the entire viewing area of the digitizer to a 240-by-240 array of real intensities. The actual beam image is usually only a portion of this array. The BCS software is used to locate the centroid of the image, determine the size of the pixels, and define a rectangular aperture enclosing the image. This information can be used to extract a 25-by-25 image array, which is directly comparable to the CIRCE2-generated array.

The dimensions of the aperture used to extract the BCS image array are used as the input target dimensions for the CIRCE2 calculations as are the other pertinent parameters from the specific test configuration. The slope error determined by the code that matches the peak power of the image data is used as the starting point for a series of computer runs. In each run (a minimum of four are done), the slope error is varied by half a milliradian. The range is selected so that the initial slope error is not one of the endpoints.

The resultant arrays are put into a spread sheet along with the extracted image array. Each array is normalized by its maximum value and an array of differences between the measured and calculated values is created for each slope error increment. A statistical figure-of-merit for the goodness of the fit is then calculated by computing the square root of the sum of squares (RSS) of the elements in each array of differences. Figure 3 is an example of the graph of the RSS difference versus slope error. The slope error based on matching peak power was calculated at 2.62 mr. A fourth-order polynomial curve fit of the data points was made to find the

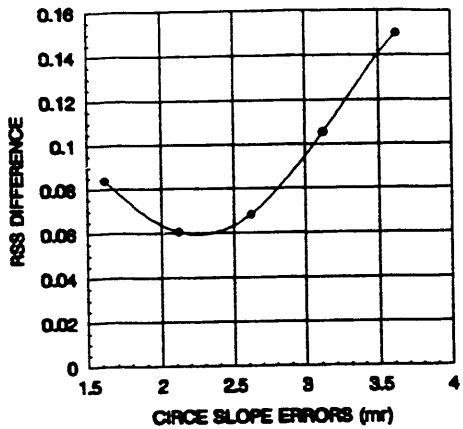


Figure 3. Example of RSS Difference graph

lowest value for the RSS difference which is approximately 2.25 mr. This curve is for the SKI single-element stretched-membrane dish and will be discussed in more detail in the next section.

5. Testing At Sandia

Three unique test programs have been undertaken at Sandia and they employ the test equipment and analysis methodology discussed above. While these on-sun tests all involved dish concentrators, these methods could also be applied to heliostats.

5.1 Single Element Stretched Membrane Dish

As part of an ongoing development program, Solar Kinetics, Inc. of Dallas, Texas, fabricated and installed a 7-meter-diameter dish (Figure 4) for testing at the NSTTF[6,7,8]. This was an intermediate-scale prototype for demonstrating an optical element constructed of a single metal membrane with an unattached polymer reflective membrane.

A series of tests was done with the BCS to determine the optimal vacuum required to hold the membrane shape and the resulting focal length. Optimum results were defined by the highest peak flux and smallest beam size. For a fixed vertex-to-target distance, the vacuum pressure was varied from 3.5 to 7 inches of water. At each increment, the membrane was allowed to stabilize, and a series of BCS images was taken. Once the best vacuum pressure was found, the vertex-to-target distance was varied until the best image was found. Analysis of the images determined a peak flux of 5168 kW/m^2 at a f/D of 0.609 and a vacuum of 0.011-

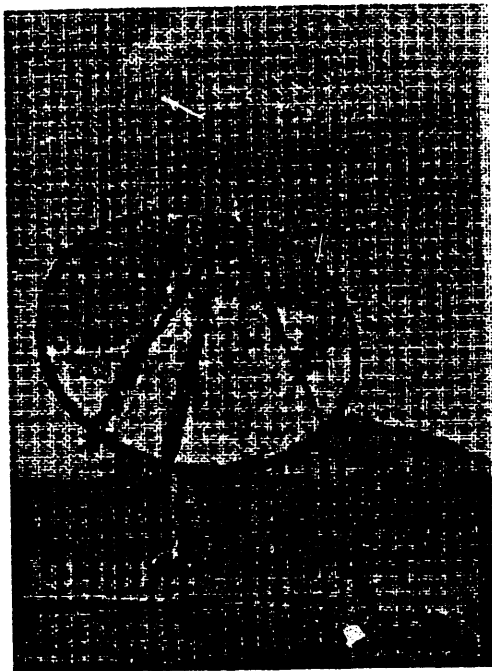


Figure 4. The 7-Meter Single-Element Stretched-Membrane Dish

bars. The total power of the dish as measured with the BCS was approximately 22.6 kW which agreed well with the 23.3 kW measured with cold-water calorimetry.

For input into CIRCE2, the coordinate system used originated at the vertex of the dish (Figure 5). Since the dish points directly at the sun, the normal and aim-point vectors are the same and both point in the direction of the sun unit vector. A 16.6 % shadow/blockage factor was used, based on the amount of the reflective area of the dish the

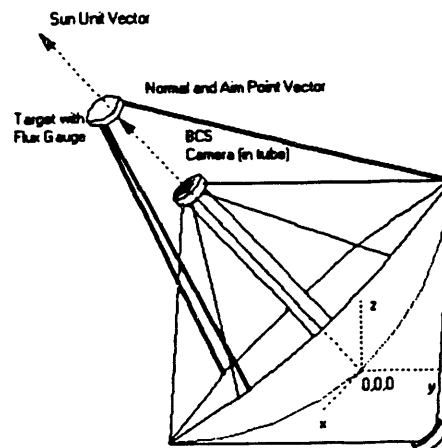


Figure 5. 7-Meter Stretched Membrane Dish Test CIRCE2 Configuration

receiver, struts, and spokes covered.

As reported earlier, the CIRCE2 slope error result for matching peak fluxes was 2.6 mr. Again, Figure 3 illustrates that the RSS difference yields a slope error of 2.3 mr. The optical characteristics of the dish closely adhered to the design goals of an f/D of 0.6 and a slope error of 2.0 mr[9].

5.2 Stretched-Membrane Facets

Another development program underway at Sandia is the Faceted Stretched-Membrane Dish Program. Two contractors, Science Applications International Corp. (SAIC)[10] and Solar Kinetics, Inc. (SKI)[11], fabricated prototype facets, which were tested on-sun at Sandia (Figure 6).



Figure 6. On-Sun Testing of a Stretched-Membrane Facet

Both 3.5-meter facets were mounted in a frame with integral focus controls. The facets were tested at three focal lengths (9.5, 10, and 10.5 meters). For each test, the focus control was set according to the instructions supplied by the fabricator. The facet was positioned with a fork lift on a grid marked on the ground of the test site so that the reflected beam was striking the target. Measurements from the bottom edge of the facet mounting frame to the grid provided input to calculations to determine the facet vertex-to-target distance. The facet position was adjusted until the calculated distance was close to the desired focal length and a series of BCS images was made. This process was repeated for both facets at each design focal length. Table 2 summarizes the results from the tests.

One set of test results for both facets at each focal length was analyzed with CIRCE2. The facet location measurements were used to calculate the facet normal for input into the program. Sun

Table 2.
Stretched-Membrane Facet Test Results

Test Number	Design Focal Length (m)	Test Focal Length (m)	Peak Flux (kW/m ²)
SAIC			
H0121144	10.50	10.68	416
H0121213	10.50	10.48	338
H0121224	10.50	10.62	389
H0151209	10.00	9.96	342
H0151223	10.00	10.05	357
H0151232	10.00	10.01	339
H0231122	9.50	9.56	355
H0231136	9.50	9.46	334
H0231148	9.50	9.55	346
H0231201	9.50	9.59	347
H0231210	9.50	9.65	365
H0231218	9.50	9.69	368
SKI			
H0251155	10.50	10.42	784
H0251205	10.50	10.55	798
H0251212	10.50	10.55	843
H0251220	10.50	10.60	638
H0251228	10.50	10.66	797
H0281129	10.0	10.10	1163
H0301145	10.0	10.28	1090
H0301154	10.0	10.02	1186
H0301208	9.50	9.55	543
H0301218	9.50	9.48	755
H0311031	9.50	9.76	645
H0311039	9.50	9.98	921

position was determined from the time and date. The coordinate system used is shown in Figure 7.

The procedure used in the analysis was the same as above. A slope error was determined based on peak power and used to provide a base for the 5 mr intervals in the RSS difference. Graphs of the difference versus slope error were used to determine the calculated slope error with the least difference. The analysis results are summarized in Table 3.

The results of the tests indicated both facets were capable of meeting the design goal of 2.5-mr[12]. Both facets are still in the development stage and the lessons learned during these tests will help improve the performance.

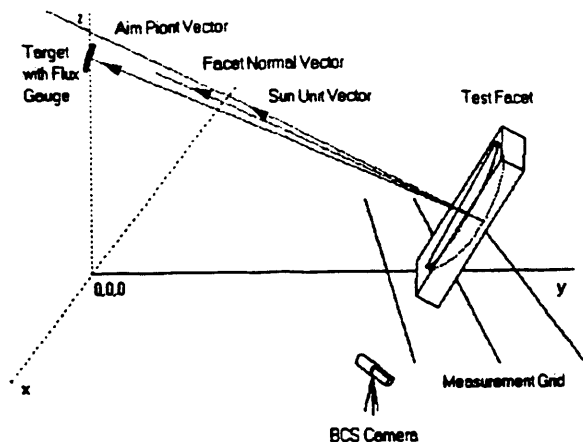


Figure 7. Stretched-Membrane Facet Test CIRCE2 Configuration

Table 3.
CIRCE2 Analysis Results For The Stretched-Membrane Facets

Design Focal Length (m)	Peak Flux Matching Slope Error (mr)	RSS Difference Slope Error (mr)	Average Peak Flux (kW/m ²)
SAIC			
10.5	2.1	2.2	381
10.0	2.7	3.0	346
9.5	2.7	3.0	353
SKI			
10.5	1.5	1.6	772
10.0	1.2	1.2	1146
9.5	1.8	1.9	716

5.3 NASA STAR Facet Testing

The final testing to be discussed here is the reimbursable tests done for NASA[13]. The Solar Thermal Advanced Receiver (STAR) facets are being developed as part of the solar dynamic power system for the Space Station Freedom. Each composite facet is a $1 \times 1 \times 1$ -meter triangle with a circular radius of curvature. Twenty four facets are used in each of nineteen hexagonally shaped panels for the concentrator. In preparation for this test program, Sandia built a solar tracking truss capable of supporting a complete panel. To date, only the facets have been tested (Figure 8)[14].

Five facets were tested at three vertex-to-target distances specified for each facet by NASA.

During testing, a facet was mounted on the truss at a NASA-specified angle to simulate a facet located

offset to the concentrator vertex. The truss would track the sun at an offset angle so that the image was centered on the target. A series of BCS images was taken for each distance, and test results are shown in Table 4.

Tracking the sun with the truss meant that the sun was always vertically above the target. With the CIRCE2 coordinate system origin at the vertex of the facet, the aim point-vector was from the vertex to target and the facet normal was midway between the aim point and the sun unit vector (Figure 9).

A CIRCE2 analysis was done for one data set for each facet. The results of the analysis are summarized in Table 5. One facet, 10/30-2, was not measured near its focal point. As a result, the image intensities were low and neither slope error method yielded reliable results.

This series of tests illustrates why the uniform slope error should be considered a figure-of-merit rather than a real value. The first two examples in this document had very symmetrical images. These facets were early prototypes that varied in surface quality and uniformity. As a result, the images varied greatly in their shape, and the slope error was not uniform (Figure 10). While CIRCE2 did

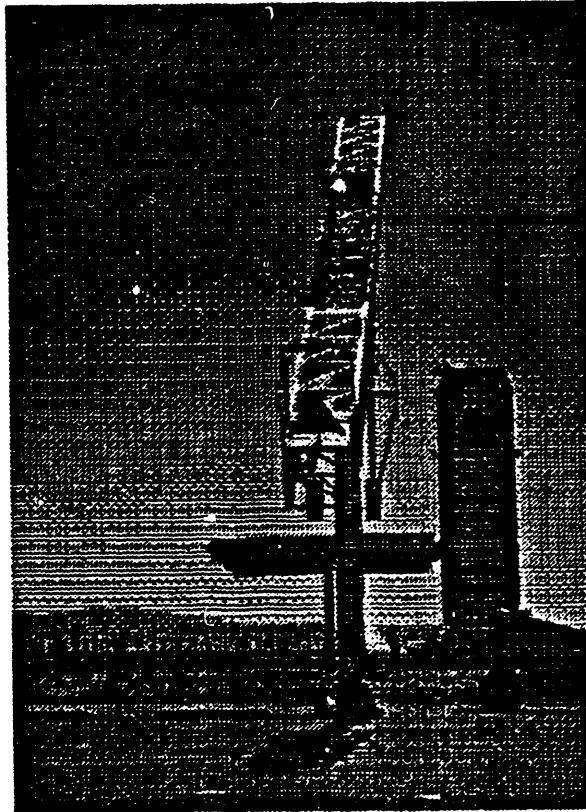


Figure 8. NASA STAR Facet On-Sun Testing With Central Receiver Test Facility In The Background

Table 4.
The NASA STAR Facets Test Results

Facet ID.	Facet-to-Target Distance (m)	Offset Angle (degrees)	Total Power (kW)	Peak Flux (kW/m ²)
10/30-2	11.68	15.11	0.359	6.1
	12.19	15.17	0.352	6.6
	12.70	15.12	0.361	7.6
5/11-S	14.27	5.47	0.277	12.5
	14.68	5.46	0.286	12.7
	15.18	5.46	0.296	15.5
REP #1	13.01	34.94	0.293	16.9
	13.52	34.95	0.250	14.4
	14.03	34.82	0.231	17.2
REP #2	11.68	4.65	0.321	21.2
	12.19	4.64	0.277	20.7
	12.70	4.62	0.217	16.7
ST-011	15.86	40.01	0.285	11.7
	15.76	39.89	0.294	11.3
	14.85	39.9	0.308	11.5

not predict the nonsymmetrical shape or varying slope error, the RSS difference would determine a slope error that approached an average value for the facet. Another way of looking at the method is if the intensity arrays were used to generate three-dimensional shapes, the RSS difference would determine a slope error so that the volume of the calculated shape would approach the volume of the actual shape. The contours of the shapes would not necessarily match, only the volume. This can be seen in the two graphs in Figure 10. In one case, 5/11-S, the slope error changes from 2.0-mr. to 1.5-mr., while for ST-011 the error changes from 0.6-mr. to 1.4-mr. For both examples, the profile

Table 5.
CIRCE2 Analysis Results NASA STAR Facets

Facet ID	Peak Flux Matching Slope Error (mr)	RSS Difference Slope Error (mr)
10/30-2	1.0 (approx.)	n/a
5/11-S	2.0	1.5
REP#1	1.0	1.3
REP#2	1.9	1.3
ST-011	0.6	1.4

shapes of the calculated lines remain symmetrical -- their breadth changes (Peak to RSS) to match the area under the actual image profile. In this manner, a figure-of-merit slope error can be developed for comparison of the facets.

6. The Future

The successful completion of these tests at the NSTTF has helped establish that

- o the prototype concentrators for the DOE Distributed Receiver Development Program have achieved the design goals with respect to optical performance,
- o the ability to predict flux distributions with CIRCE2 has established its usefulness as an analytical tool (this ability is less with lower quality concentrators),
- o a valid test method has been developed for

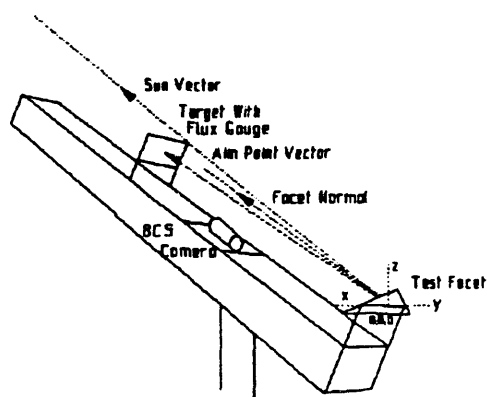


Figure 9 NASA STAR Facet Test CIRCE2 Configuration

the solar concentrators, which provides a basis for comparison, and

- o the test equipment and analysis method developed at Sandia can be used for a wide range of test configurations.

The Concentrator Receiver Development Program is continuing with the development of commercial prototypes of both the stretched-membrane faceted and the single-element membrane dishes. In addition, Sandia has helped evaluate the Cummins LEC-460 Dish-Stirling system. We anticipate that we will continue to support this commercialization effort.

With that in mind, we are continuing to improve the test equipment and analysis methods. Additional water cooled targets and flux gauges have been procured to expand the range of test configurations. An in-depth error analysis of the

BCS is being performed to more accurately define the error band and indicate areas where improvements should be made.

Two areas are being considered for the RSS difference method. As part of the data analysis, the current technique for creating the 25-by-25 measured image array extracts single pixel values. A program that extracts averaged values should

improve the technique. We are now using the RSS method, yet there might be another more effective comparison method. At the same time these questions are being asked, we must evaluate their value, remembering the slope error is only a figure-of-merit presently accepted with two significant digits. A significant effort to improve performance at the third significant digit would be unjustified.

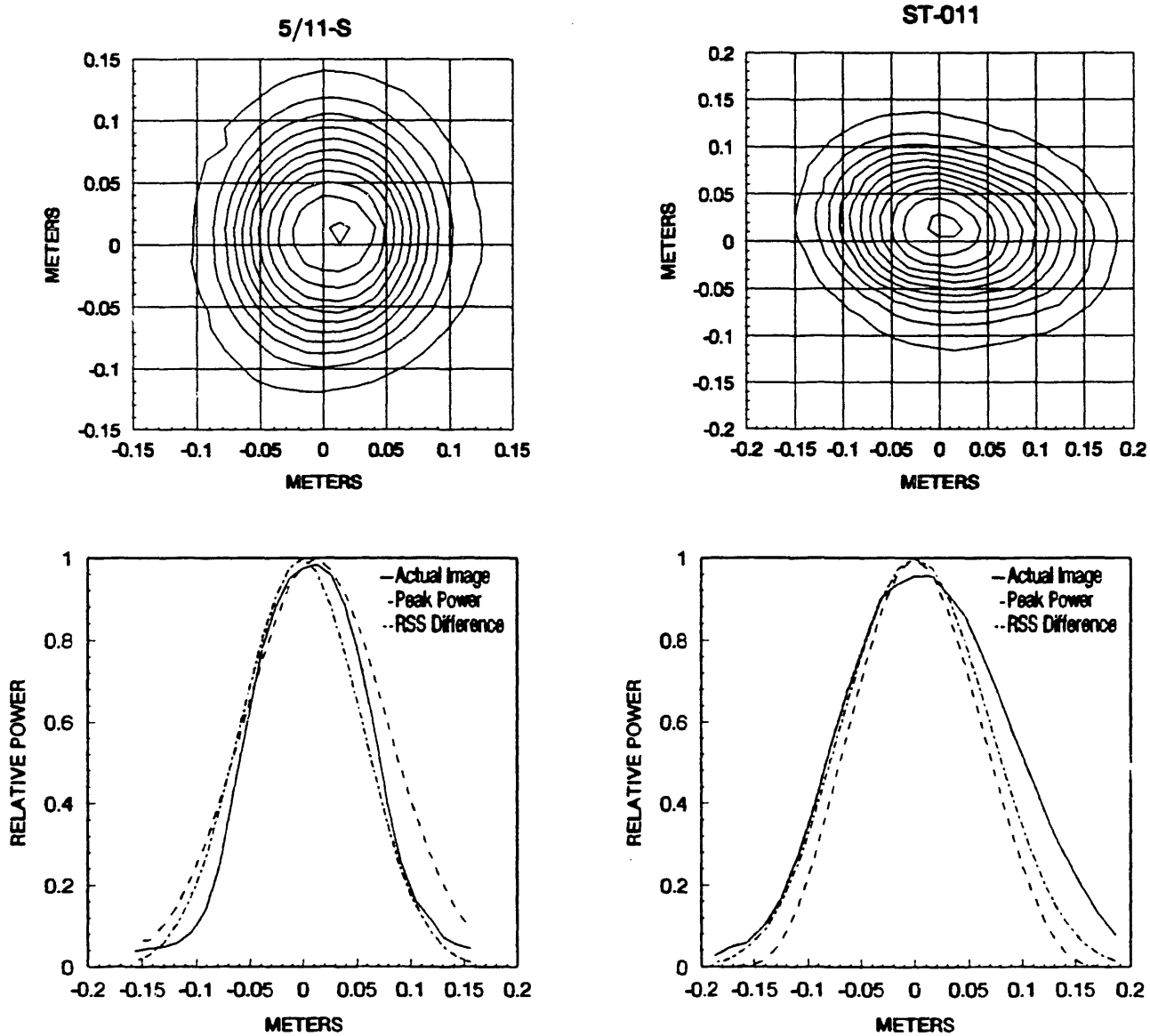


Figure 10 NASA STAR Facet Shape Comparison

7. References

1. Maxwell, C. W., and J. T. Holmes, *Central Receiver Test Facility Experiment Manual*, SAND 86-1492, Sandia National Laboratories, Albuquerque, NM, Reprinted March 1988.
2. *National Solar Thermal Test Facility*, SAND 89-1691, Sandia National Laboratories, Albuquerque, NM, 1989.
3. Biggs, F., and C. N. Vittitoe, *The HELIOS Model for the Optical Behavior of Reflecting Solar Concentrators*, SAND 76-0347, Sandia National Laboratories, Albuquerque, NM, March, 1979.
4. Ratzel, A. C., and B. D. Boughton, *CIRCE.001: A Computer Code for Analysis of Point-Focus Concentrators with Flat Target*, SAND 86-1866, Sandia National Laboratories, Albuquerque, NM, February, 1987.
5. Romero, V. J., *CIRCE.002: A Computer Code for Analysis of Point-Focus Solar Collector Systems*, SAND 90-XXXX, Sandia National Laboratories, Albuquerque, NM, to be published.
6. *Development of a Stretched-Membrane Dish*, SAND 88-7031 (Solar Kinetics, Inc., Dallas, Texas), Sandia National Laboratories, Albuquerque, NM, October 1989.
7. *Development of a Stretched-Membrane Dish-Phase I*, SAND 88-7035 (Solar Kinetics, Inc., Dallas, Texas), Sandia National Laboratories, Albuquerque, NM, March 1989.
8. *Development of a Stretched-Membrane Dish-Phase II, Task 2. Topical Report*, SAND 90-7036 (Solar Kinetics, Inc., Dallas, Texas), Sandia National Laboratories, Albuquerque, NM, July, 1991.
9. "Statement of Work Stretched-Membrane Dish Collector Development Project", Sandia Contract No. 53-9663, Sandia National Laboratories, June 1, 1986.
10. *Facet Development for a Faceted Stretched-Membrane Dish by SAIC*, SAND 91-7008 (Science Applications International Corp.), Sandia National Laboratories, Albuquerque, NM, to be published.
11. *Facet Development for a Faceted Stretched-Membrane Dish by Solar Kinetics, Inc.*, SAND 91-7009 (Solar Kinetics, Inc., Dallas, Texas), Sandia National Laboratories, Albuquerque, NM, March 1989.
12. "Statement of Work Faceted Stretched-Membrane Dish Development Project", Sandia Contract No. 42-9814, Sandia National Laboratories, June 7, 1989.
13. Mancini, T.R., C. P. Cameron, and V. R. Goldberg, *NASA SCAD Concentrator Terrestrial Testing Feasibility Study*, Report to NASA Lewis Research Center, Contract No. C-31006-J, September 1988.
14. Grossman, J. W. T. R. Mancini, R. M. Houser, and W. W. Erdman, *Task 3 Report: On-Sun Test and Evaluation of The NASA STAR Facets*, Report to NASA Lewis Research Center, Contract No. C-31006-J, June, 1991.

END

DATE
FILMED

3 / 4 / 92